Cellular Signalling 53 (2019) 316–326

Contents lists available at ScienceDirect

Cellular Signalling

journal homepage: www.elsevier.com/locate/cellsig

Sterol regulatory element binding protein (SREBP) -1 mediates oxidized low-density lipoprotein (oxLDL) induced macrophage foam cell formation through NLRP3 inflammasome activation

Johnna F. Varghese, Rohit Patel, Umesh C.S. Yadav*

Metabolic Disorders and Inflammatory Pathologies Laboratory, School of Life Sciences, Central University of Gujarat, Gandhinagar, Gujarat 382030, India

ARTICLE INFO

Keywords:
Atherosclerosis
Macrophage foam cells
SREBP-1
Inflammasome
Monocytes
Oxidized low-density lipoprotein

ABSTRACT

Macrophage foam cell formation (FCF) has long been known to play a critical role during atherosclerotic plaque development. In the presence of atherogenic molecules such as oxidized low-density lipoprotein (oxLDL) macrophages accumulate massive amounts of lipid through uptake. However, in the presence of oxLDL mechanism of dysregulated lipid homeostasis in the macrophages remains largely unknown. Herein we have investigated the role of Sterol regulatory element binding protein (SREBP)-1 in oxLDL-induced inflammation and altered lipid homeostasis in macrophages. The U937 monocytes and monocyte-derived macrophages (MDMs) were stimulated with different doses of oxLDL. MTT assay to study the effect of oxLDL on cell viability, Oil-Red-O (ORO) staining to observe cytosolic lipid accumulation, semi-quantitative PCR and Western blotting to analyze mRNA and protein expressions, respectively, and spectrophotometric assay to measure the lipid synthesizing enzyme's activity were performed. Our results indicate that oxLDL increased proliferation in monocytes and decreased the viability in MDMs in a time- and dose-dependent manner. The oxLDL (100 μg/ml) enhanced lipid accumulation *via* increased expressions of SREBP-1 and its downstream proteins such as fatty acid synthase (FAS) and 3-hydroxy-3-methylglutaryl-CoA reductase (HMGCR) at both RNA and protein levels in monocytes as well as in MDMs. Inhibiting SREBP-1 by a synthetic inhibitor prevented excessive lipid accumulation by downregulating the expression of its downstream proteins. Further, oxLDL increased reactive oxygen species (ROS) levels, NLRP3 inflammasome activation and active interleukin 1β (IL-1β) release in both the cell types. The oxLDL-induced NLRP3 could be responsible for SREBP-1 and downstream proteins overexpression as siRNA silencing of NLRP3 decreased SERBP-1 levels. In summary, we have demonstrated that SREBP-1 could be a key player in oxLDL-induced excessive lipid accumulation leading to macrophage FCF *via* ROS-mediated NLRP3/IL-1β/SREBP-1 pathway.

1. Introduction

Monocytes and macrophages, the central regulators of the innate immune system, have been recognized as key players in chronic cardiovascular diseases such as atherosclerosis. The phenomenon of macrophage foam cell formation (FCF) has been regarded as a critical event in the development of atherosclerotic plaque, a leading cause of cardiovascular diseases (CVDs). American Heart Association (AHA) estimated that approximately 17.3 million global deaths are caused due to CVDs every year [1]. The role of several risk factors such as hyperglycemia, hyperinsulinemia, dyslipidemia and obesity in causing atherosclerosis is now well established [2]. A positive correlation between total or LDL cholesterol levels, one of the major risk factors, and atherosclerosis has been clinically well established [3], although a few recent reports have refuted the claim that LDL alone could induce atherosclerosis [4,5]. However, oxidation product of LDL, also known as oxidized-LDL (oxLDL), has been identified as potent atherogenic molecule [6]. The oxLDL uptake by macrophages and their subsequent

Abbreviations: FCF, foam cell formation; oxLDL, oxidized low-density lipoprotein; SREBP-1, sterol regulatory element binding protein-1; MDMs, monocyte-derived macrophages; ORO, Oil Red O; FAS, fatty acid synthase; HMGCR, 3-hydroxy-3-methylglutaryl-CoA reductase; ROS, reactive oxygen species; IL-1β, interleukin 1β; NLRP3, nucleotide binding oligomerization domain (NOD), leucine-rich repeats (LRR) containing family, pyrin domain (PYD) containing 3; PMA, phorbol 12-myristate 13-acetate; NAC, N-Acetyl Cysteine; GAPDH, Glyceraldehyde-3-phosphate dehydrogenase; DCFDA, Dichlorofluorescin diacetate; DMSO, Dimethyl sulfoxide, 4′,6-diamidino-2-phenylindole (DAPI), 1,4-diazabicyclo[2.2.2]octane (DABCO)

* Corresponding author.
E-mail address: umeshyadav@cug.ac.in (U.C.S. Yadav).

https://doi.org/10.1016/j.cellsig.2018.10.020
Received 3 July 2018; Received in revised form 26 October 2018; Accepted 29 October 2018
Available online 31 October 2018
0898-6568/

transformation into foam cells is a hallmark of early atherosclerotic lesions [7]. Evidently, oxLDL (and not native LDL) has been found to drive monocytes differentiation into macrophages [8]. The dysregulated lipid metabolism in macrophages resulting in excessive lipid accumulation has been implicated in maladaptive immune response and atherosclerotic plaque development [9]. Several studies have purported well-defined mechanisms that cause FCF including persistent exposure of monocytes to elevated levels of modified LDLs in circulation. These modified lipids increase the expression of a plethora of scavenger receptors such as type 1 and II (SR-AI and II), cluster of differentiation 36 (CD36) *etc.*, and decrease the expression of efflux proteins such as ATP binding cassette transporter A1 and G1 (ABCA1 and ABCG1) in macrophages leading to increased lipid accumulation [9–12]. Although the function of scavenger receptors as lipid uptake propellers and decreased efflux transporters have been implicated in FCF, the dysregulated *de novo* lipid synthesis in monocytes and MDMs in the presence of modified LDLs remains unexplored.

Lipid homeostasis is maintained and regulated by a helix-loop-helix leucine zipper family of transcription factors. The sterol regulatory element binding proteins (SREBPs) belongs to this family, which transcribe enzymes involved in endogenous synthesis of cholesterol, fatty acids and phospholipids [13]. Out of broadly two isoforms, SREBP-1 is responsible for both fatty acid and cholesterol synthesis whereas SREBP-2 exclusively regulates cholesterol synthesis. Altered expression of SREBP in epicardial adipose tissue illustrates its contribution in severity of coronary artery disease and type-2 diabetes through poor control of lipid synthesis [14]. Further, during dysregulated metabolic condition, overexpression of lipid synthesizing enzymes such as fatty acid synthase (FAS) and 3-hydroxy-3-methylglutaryl-CoA reductase (HMGCR) have also been implicated in excessive lipid synthesis in the cells [15]. Furthermore, studies have also indicated that dysregulated lipid synthesis in the cells leads to foam cell phenotype [16]. Thus, we hypothesized that exacerbated *de novo* lipid synthesis in the monocytes and MDMs, besides excessive cytosolic lipid content including modified-LDL, may contribute towards FCF [17]. Since oxLDL has been shown to increase ROS levels and activate NLRP3 inflammasome and subsequently release biologically active IL-1β [18], we have investigated whether oxLDL-induced NLRP3 inflammasome could activate SREBP-1 and its downstream proteins leading to excessive *de novo* lipid synthesis in monocytes and MDMs.

2. Materials and methods

2.1. Cell line and reagents

The U937 cell line was obtained from ATCC (Manassas, VA, USA) and cultured in RPMI 1640 media supplemented with 10% fetal bovine serum (FBS) procured from Gibco Life Technologies (Grand Island, NY, USA). Antibodies against SREBP-1, HMGCR and caspase-1 were obtained from Santa Cruz Biotechnology (Dallas, TX, USA), Glyceraldehyde-3-phosphate dehydrogenase (GAPDH), Tata Binding Protein (TBP), IL-1β and FAS from cell signaling technology (Denver, CO, USA), and NLRP3 from Abcam (Cambridge, MA, USA). Specific siRNA for silencing NLRP3 (Cat. No. SI05050801) or scrambled siRNA (Cat No. 1027280) and HiPerfect transfection reagent were purchased from Qiagen (Hilden, Germany). HRP conjugated anti-rabbit and anti-mouse secondary antibodies were obtained from BioRad (Hercules, CA, USA). Enhanced chemiluminescence (ECL) system and its associated components such as luminol was from Sisco Research Laboratories (SRL) Pvt. Ltd. (Mumbai, MH, India) and p-coumaric acid, phorbol 12-myristate 13-acetate (PMA), Fatostatin, N-Acetyl Cysteine (NAC), acetyl coenzyme A, malonyl CoA, NADP, Oil Red O (ORO) Stain, 4′,6-diamidino-2-phenylindole (DAPI), 1,4-diazabicyclo[2.2.2]octane (DABCO) were from Sigma (St. Louis, Missouri, USA), Trizol from (Life Technologies, Waltham, MA USA) and native LDL was obtained form Prospec-Tany TechnoGene Ltd. (Rehovot, Israel). All other reagents were of analytical grade procured from SRL Pvt. Ltd.

2.2. Cell culture and macrophage differentiation

U937 cells were cultured in the incubator (ESCO Micro PTE. LTD., Changi, Singapore) with 5% CO_2, 95% humidity and 37 °C temperature. Monocytes were seeded in the culture dishes as required and incubated with 10 nM PMA (final concentration) for 72 h. The differentiation of the monocytes into macrophages was confirmed by morphological examination and assessment of macrophage specific cell surface receptor CD36. After differentiation, the MDMs were used in subsequent experiments.

2.3. Oxidation of LDL

Native LDL was oxidized using $CuSO_4$ method with a final concentration of 5 μM [19]. Oxidation of LDL was confirmed by agarose gel electrophoresis and TBARS kit (HiMedia Laboratories; Mumbai, MH, India) [20]. The oxLDL was stored at 4 °C in airtight vials and used within a month. Protocol for oxidation was standardized followed by confirmation for each batch with the above-mentioned methods.

2.4. MTT assay

Approximately 1.0×10^4 U937 monocytes and MDMs were seeded in 96-well plates. MDMs were incubated for 24 h and allowed to adhere. The cells were serum-starved (1% FBS) overnight, followed by stimulation with different doses of oxLDL and incubated for different time intervals (24 and 48 h). At the end of incubation 10 μl of 3-(4,5-dimethylthiazol-2-yl)-2,5-diphenyltetrazolium bromide (MTT) (5 mg/ml) was added into each well and incubated for additional 4 h. The media was carefully aspirated out, 100 μl of dimethyl sulfoxide (DMSO) was added to dissolve the formazan crystals. The absorbance was measured at 570 nm using Synergy H1 Hybrid microplate reader (Winooski, VT, USA).

2.5. Oil Red O staining

Approximately 1.5×10^5 monocytes were seeded in 24-well plates and differentiated as described above. Once differentiated the cells were serum-starved with or without fatostatin (20 μM) and stimulated with oxLDL (100 μg/ml) or IL-1β (10 ng/ml) for 24 h. At the end of incubation, cells were fixed in 2% paraformaldehyde for 1 h and ORO staining was performed as described [21]. Quantification of the lipid content in macrophages was carried out by eluting the dye from each well with 100% isopropanol and absorbance was measured spectrophotometrically at 500 nm as described earlier [21].

2.6. Semi-quantitative PCR

One microgram of total RNA was reverse transcribed to cDNA in a final volume of 20 μl using cDNA synthesis kit from BioRad (Hercules, CA, USA). Primers for selected transcripts such as SREBP-1 (Forward: 5′ AGTGACTTCCCTGGGCCTATT 3′ Reverse: 5′TGGACGGGTACATCTTCA ATGG3′), HMGCR (Forward: 5′GCAGGACCCCCTTTGCTTAGAT3′ Reverse: 5′TCGAGCCAGGCTTTCACTTC3′), FAS (Forward: 5′GAACGG CAACCTGGTAGTGA3′ Reverse: 5′CCTGGAAATGAGGGCCGTAG3′) were obtained from imperial life science (Gurugram, HR, India) and NLRP3 (Forward: 5′GCTCTGTGATCCTTCCGGTG3′ Reverse: 5′CTGGT GTCTTCCTCACCCTG3′), and GAPDH (Forward: 5′GCCTTCCGTGTCCC CACTGC 3′ Reverse: 5′CAATGCCAGCCCCAGCGTCA 3′) from Eurofins (Brussels, Belgium). PCR was performed with 3 μl of cDNA in a final volume of 25 μl PCR reaction mixture containing HiBuffer, $MgCl_2$, dNTP and Taq Polymerase (HiMedia Laboratories, Mumbai, MH, India) and subjected to initial denaturation of 94 °C for 5 min, followed by 30 cycles of denaturation at 94 °C for 30s, annealing Tm varied according to primer sequences for 45 s and extension at 72 °C for 1 min, followed by final extension at 72 °C for 5 min using Veriti 96-well Thermal Cycler (Applied Biosystems, CA, USA). The PCR products were analyzed using 1.5% agarose gel containing ethidium bromide [22]. Densitometric analysis of the bands was performed using Alpha imager software (San Jose, CA, USA).

2.7. Western Blotting

Approximately 1×10^6 cells were seeded in 35 mm-plates for obtaining whole cells lysate or nuclear and cytosolic fractions. Cells were serum-starved overnight, pretreated with Fatostatin (20 μM) for 2 h or *N*-acetyl cysteine (5 mM) for 6 h where required, and stimulated with oxLDL (100 μg/ml) or IL-1β (10 ng/ml) for different durations as required for the given experiments. Subsequently, cells were collected, washed with ice cold 1× PBS and were either lysed for whole cell lysates or processed for extraction of nuclear and cytosolic fractions [23]. Protein concentrations were determined using Bradford reagent and equal amount of protein was resolved on 10% sodium dodecyl sulfate-polyacrylamide gel electrophoresis (SDS-PAGE). Separated proteins were then transferred to PVDF membranes, which were then blocked by incubating in blocking buffer containing 5% non-fat skim milk powder or bovine serum albumin (HiMedia Laboratories, Mumbai, MH, India). The membranes were probed with primary antibodies overnight at 4 °C. The membranes were washed and incubated with HRP conjugated secondary antibodies for 2 h at room temperature. The protein bands were detected by ECL method and densitometry was performed using the Alpha imager software (San Jose, CA, USA).

2.8. siRNA transfection of U937 cells

Approximately 1.5×10^5 cells/well in 100 μl of serum-free media were seeded in a 24-well plate. Subsequently, 100 nM of NLRP3 siRNA or scrambled siRNA were mixed with 6 μl of HiPerfect transfection reagent in serum-free media (100 μl) and added to each well followed by incubation for 6 h. Subsequently 400 μl of complete media was added and incubated further for 72 h. The siRNA-mediated silencing of NLRP3 was assessed by Western blotting as described earlier.

2.9. Determination of enzyme activity

The enzyme activity of FAS in different groups was determined in the cell lysates prepared by sonication. The catalytic reaction for each sample was carried out in 1 ml of reaction volume containing 100 μmol of potassium phosphate buffer (pH 6.5); 0.5 μmol NADPH; 75 nmol malonyl-CoA; 50 nmol acetyl-CoA and 500 μg of protein lysate. Reaction was started by adding the substrates and absorbance was based on the oxidation of NADPH, where a decrease in absorbance at 340 nm due to conversion of NADPH in to $NADP^+$ during the reaction indicated FAS activity [24]. Blank contained cell lysate without the substrates in an identical cuvette. The changes in absorbance were measured at 340 nm using Hitachi U-2900 spectrophotometer (Tokyo, Japan).

2.10. Immunocytochemistry

Approximately 1.5×10^5 cells/well were seeded on the coverslips in a 24-well plate. Cells were serum-starved overnight, stimulated with oxLDL (100 μg/ml) for 6 h. Cells were subjected to fixation for 1 h in 2% buffered paraformaldehyde and further processed for immunofluorescence staining [21]. The stained cells were observed using fluorescent microscope (Olympus BX53 model, Tokyo, Japan) at 400× magnification and images were captured with camera (ProgRes C5 model of Jenoptik, Thuringia, Germany) fitted to the microscope.

2.11. Determination of ROS

Approximately 1.0×10^4 cells/well were seeded in triplicate in a 96-well plate and serum-starved overnight. Cells were washed with Krebs-ringer bicarbonate (KRB) buffer and incubated with 10 μM of 2′, 7′ dichlorofluorescin diacetate (DCFDA) for 30 min in dark. DCFDA was removed and the cells were washed twice with KRB buffer, followed by treatment with oxLDL (100 μg/ml) or H_2O_2 (1 mM; positive control). Fluorescence was measured at different time points (0, 30, 60, 180 min) at excitation/emission wavelengths of 485/530 nM, respectively, using Synergy H1 Hybrid microplate reader (Winooski, VT, USA).

2.12. Statistical analysis

Each experiment was conducted in triplicates and repeated to ensure reproducibility. Statistical analysis of the data, represented as mean ± SD, was performed using one-way ANOVA followed by Dunnet's multiple comparison and unpaired student's *t*-test (using graph-pad prism software version 5) to compare the untreated and treated samples. *p*-value at < .05 was considered statistically significant.

3. Results

3.1. OxLDL altered cell viability and induce foam cell phenotype in MDMs

Firstly, to explore the effect of oxLDL on the viability of monocytes and MDMs the cells were treated with different doses of oxLDL ranging from 0 to 150 μg/ml for 24 and 48 h followed by MTT assay. At 50, 100 and 150 μg/ml concentrations of oxLDL, an increase in percent cell viability of monocyte by 13.2%, 20.8% and 23.8% ($p < .005$) at 24 h (Fig. 1A(i)) and 33.3%, 46.7% and 46.8% ($p < .0005$) at 48 h (Fig. 1A(ii)), respectively was observed. In MDMs, the cell viability decreased by 8.4%, 11.6% and 13.5% ($p < .05$) at 24 h (Fig. 1B (i)) and by 9.2%, 15.51% and 53.4% ($p < .0005$) at 48 h (Fig. 1B (ii)), respectively. These results showed that in monocytes increasing oxLDL concentration caused increased cell growth at both the time points whereas in MDMs there was significant ($p < .0005$) decrease in cell viability at higher oxLDL concentration of 150 μg/ml at 48 h although some non-significant effect was observed at lower concentrations at both time points. Based on these data 100 μg/ml concentration of oxLDL was selected for further experiments.

Macrophages have been shown to accumulate lipids and convert into foam cells in the presence of oxLDL in atherosclerotic lesions [25]. Therefore, to determine lipid accumulation, we performed Oil-Red-O (ORO) staining after treatment of MDMs with oxLDL. A significant ($p < .05$) increase in the cytosolic lipid accumulation in MDMs, treated with 100 μg/ml oxLDL at 24 h was observed as compared to control (Fig. 1C).

3.2. OxLDL upregulated SREBP-1 and its downstream proteins at transcriptional and translational level

Since an increased lipid accumulation was observed in MDMs, to determine if it was due to SREBP-1, we next assessed the expression of SREBP-1. As shown in Fig. 2A, after oxLDL treatment a significant increase of 1.9- and 2.3-fold ($p < .005$) in the expression of SREBP-1 at mRNA level at 16 h was observed in monocytes and MDMs, respectively, compared to respective controls.

SREBP-1 is present in cytosol as precursor form and it is cleaved into mature form, a 68 kDa protein. Thus, we next assessed SREBP-1 protein, both precursor and mature forms. The whole cell lysates of monocytes and MDMs treated with oxLDL (100 μg/ml) for different time points was subjected to Western blotting. In monocytes the precursor form increased by 1.4-, 1.3- and 1.6-fold ($p < .05$) and the mature form increased by 1.3-, 2.4- and 2.8-fold ($p < .005$) (Fig. 2B) at 6, 12 and

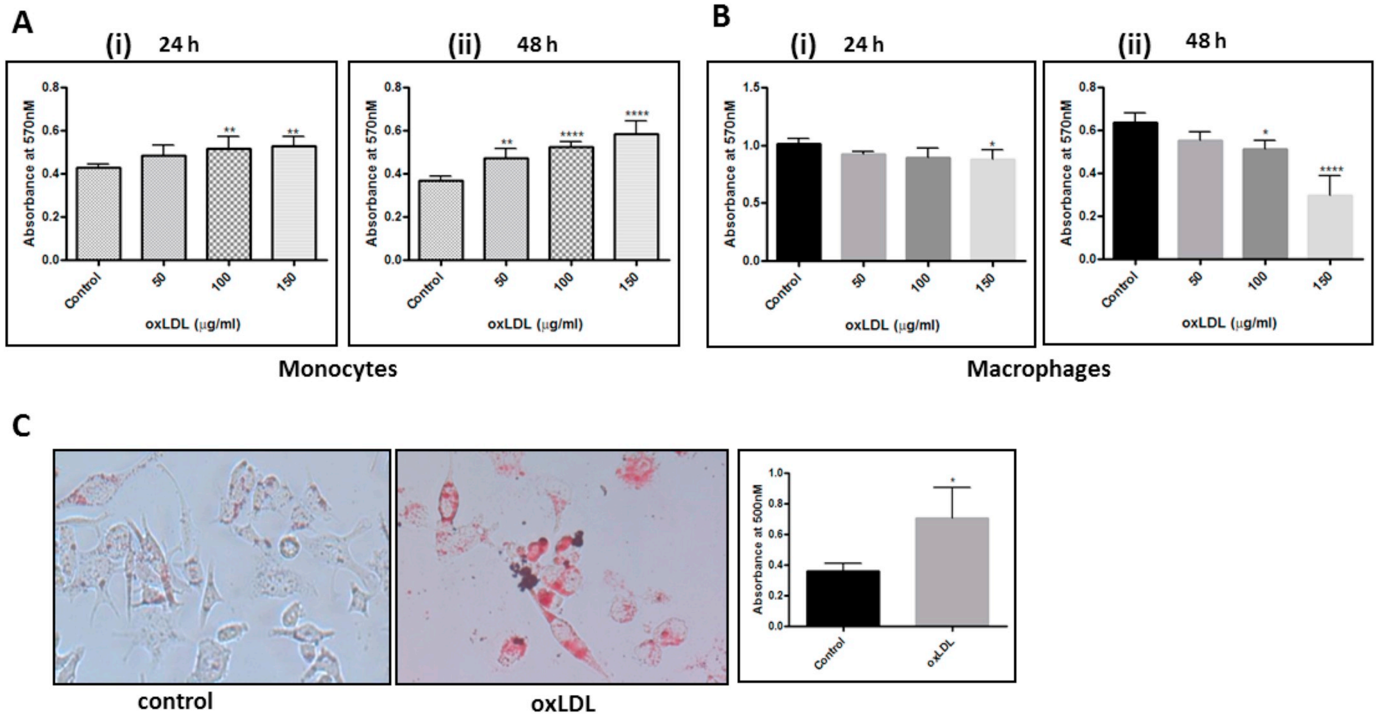

Fig 1. OxLDL altered cell viability and induce foam cell phenotype in MDMs: (A) U937 were treated with different doses of oxLDL and MTT assay was performed. The bars show mean ± SD for 24h (i) and 48 h (ii). (B) MDMs were treated with different doses of oxLDL as in U937, and MTT assay was performed. Bars show mean ± SD for 24h (i) and 48 h (ii). (C) ORO stained microscopic images of MDMs treated with 100 μg/ml of oxLDL for 24h. The bars represent mean ± SD of absorbance at 500nM of neutral lipid accumulation in MDMs at 24 h. *p < .05, **p < .005, ***p < .0005 versus respective controls.

24 h, respectively, compared to respective controls. Similarly, in MDMs the precursor form increased by 1.1-, 1.3- and 1.4-fold ($p < .05$) while mature form of SREBP-1 increased by 1.8-, 2.3- and 3.6-fold ($p < .0005$) at 6, 12 and 24 h, respectively, compared to control (Fig. 2B). Further, the mature form of SREBP-1 translocates to the nucleus where it activates the transcription of target genes. Thus, we examined the nuclear translocation of mature form of SREBP-1 in monocytes and MDMs at different time points after stimulation with oxLDL. As shown in Fig. 2C, nuclear translocation of mature SREBP-1 increased by 1.1-, 1.3- and 1.7- fold ($p < .005$) in monocytes and by 1.8-, 1.6- and 1.9-fold ($p < .005$) in MDMs, compared to respective controls (Fig. 2C). The oxLDL-stimulated nuclear translocation of mature SREBP-1 in both U937 monocytes and MDMs was further confirmed by immunocytochemistry as shown in Fig. 2D.

SREBP-1, once in the nucleus, binds to the sterol responsive elements in the promoter regions of target genes such as FAS and HMGCR and enhances their transcription. Therefore, we next examined their expression at RNA levels at 16 h in monocytes and MDMs after stimulating with oxLDL. As shown in Fig. 2E, an increased expression of FAS and HMGCR by 1.5- and 1.6-fold ($p < .05$) was observed in monocytes, while in MDMs their levels increased by 1.8- and 2.6-fold ($p < .005$), respectively (Fig. 2E).

Additionally, at the protein level FAS expression increased by 1.2- and 1.6-fold ($p < .005$), compared to control while that of HMGCR increased by 1.3- and 3-fold ($p < .005$) at 12 and 24 h, respectively (Fig. 2F) in monocytes. In MDMs, the expression of FAS increased by 1.7- and 3-fold ($p < .05$) and that of HMGCR increased by 2.2- and 3-fold ($p < .0005$) at 12 and 24 h, respectively (Fig. 2F).

These results suggest that oxLDL could increase the expression and activation of transcription factor SREBP-1 which in turn increased the expression of its target lipid synthesizing genes FAS and HMGCR enzymes in the monocytes and MDMs.

3.3. SREBP-1 inhibition prevented oxLDL induced lipid accumulation, critical component of foam cell formation

To further ascertain the function of SREBP-1 in oxLDL-mediated lipid accumulation and FCF, we inhibited SREBP-1 with fatostatin (20 μM), a well-known inhibitor of SREBP-1 [21], and examined the expression of SREBP-1 and its downstream proteins after 24 h stimulation with oxLDL. As shown in Fig. 3A, in monocytes, the expression of precursor form as well as mature form of SREBP-1 increased up to 1.4- and 1.8-fold ($p < .05$) in oxLDL-treated groups respectively as compared to control. The expression of precursor and mature SREBP-1 decreased to 0.8- and 0.6-fold in oxLDL group pretreated with fatostatin. We also found significant increase in FAS and HMGCR levels to 1.5- and 2-fold ($p < .005$), respectively, in oxLDL-treated groups as compared to respective controls, which decreased to 0.6- and 0.7-fold ($p < .05$), respectively in oxLDL group pretreated with fatostatin. Similar result was found in MDMs where precursor and mature form of SREBP-1 increased to 1.7- and 2-fold ($p < .005$) in oxLDL-treated group respectively, as compared to controls, which decreased to 0.9- and 0.6-fold ($p < .005$) in oxLDL group pretreated with fatostatin. The expression of downstream proteins FAS and HMGCR increased to 2- and 2.2-fold ($p < .05$) respectively in oxLDL treated group, as compared to control, and decreased to 0.6- and 0.9-fold ($p < .05$) respectively in oxLDL group pretreated with fatostatin. Further, fatostatin alone did not have significant effects on the precursor form of SREBP-1; however, it appreciably reduced level of mature SREBP-1, FAS and HMGCR in both the cell types.

Additionally, we determined the enzyme activity of FAS and observed that in monocytes the enzyme activity in oxLDL-treated cells increased by 3-fold ($p < .05$) when compared with control (Fig. 3B). It decreased to near control levels when cells were treated with fatostatin before stimulation with oxLDL. Similarly, in MDMs the enzyme activity in oxLDL-treated cells increased by 2-fold ($p < .05$) as compared to control, which decreased to near control levels when treated with

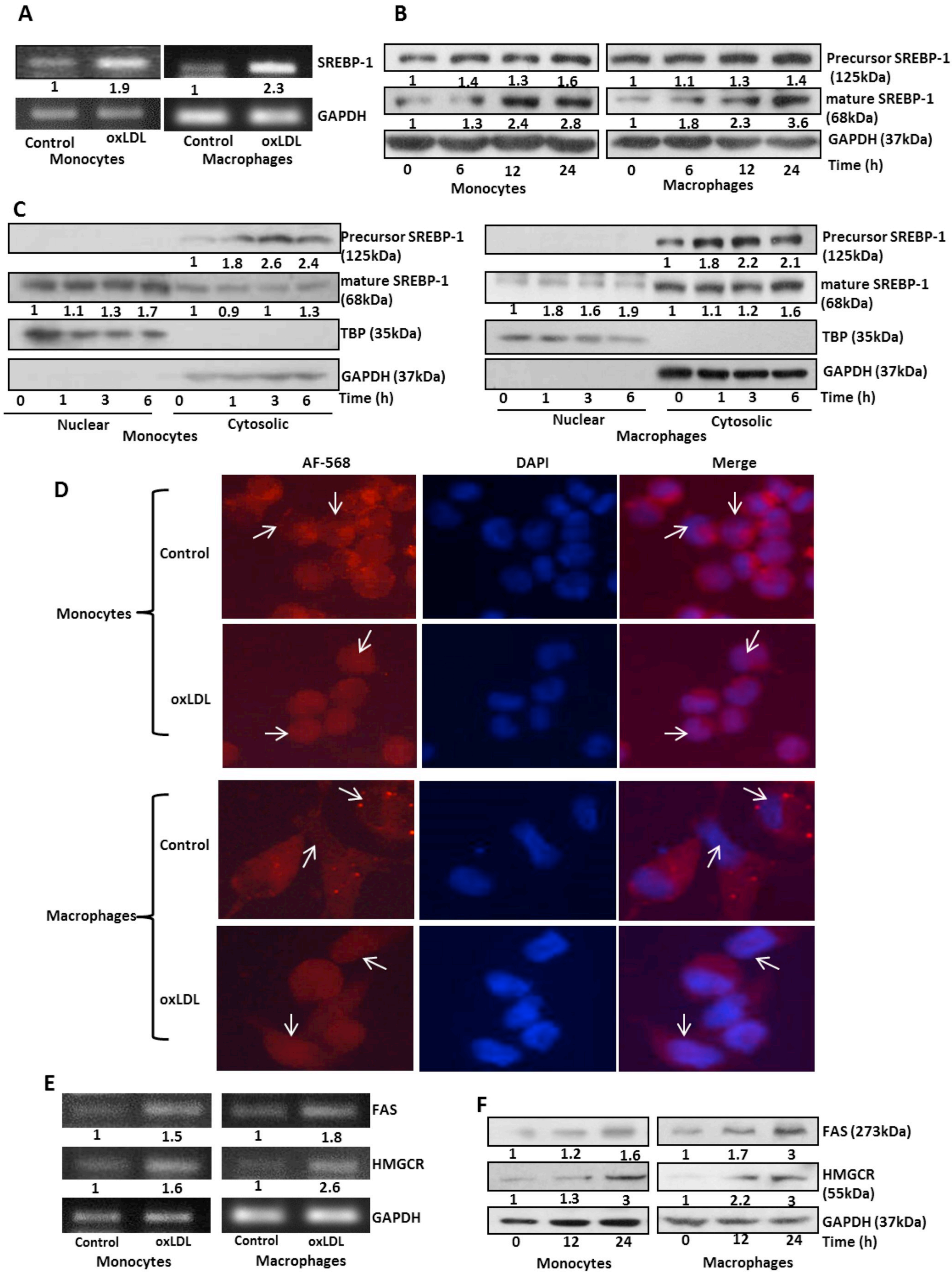

(caption on next page)

Fig 2. OxLDL upregulates SREBP-1 at transcriptional and translational levels: Monocytes and MDMs were treated with 100 μg/ml of oxLDL for different time points. (A) Representative PCR images of SREBP-1 expression at 16h. (B) Representative Western blot images of precursor SREBP-1 and mature SREBP-1 expression at 6, 12 and 24h (C) Nuclear translocation of mature SREBP-1 in monocytes and MDMs along with TBP as nuclear and GAPDH as cytosolic loading control when stimulated with oxLDL for 1, 3 and 6 h (one-way ANOVA followed by Dunnet's test). (D) Immunofluorescent images of SREBP-1 nuclear localization in monocytes and MDMs upon oxLDL stimulation for 6 h, magnification 400X. Arrows indicate the nuclear region of the cells. (E) Representative PCR images depict the mRNA expression of FAS and HMGCR in monocytes and MDMs after 16 h of oxLDL stimulation. (F) Representative Western blotting images of FAS and HMGCR expression in monocytes and MDMs stimulated with oxLDL for 12 and 24 h. Numbers below the bands indicate fold change.

fatostatin before stimulating with oxLDL (Fig. 3B). We next performed ORO staining of MDMs treated with oxLDL with or without fatostatin. In oxLDL-treated MDMs the lipid content increased by 50%, which decreased by 27.36% ($p < .005$) when cells were pretreated with fatostatin before oxLDL stimulation. Fatostatin alone could also decrease the lipid content by 19.85% ($p < .05$) when compared with control (Fig. 3C).

These results indicated that SREBP-1 inhibition in oxLDL-stimulated cells results in the decreased expression of lipid synthesizing enzymes as well as their activity resulting in decreased *in vivo* lipid synthesis and accumulation in MDMs indicating FCF inhibition.

3.4. OxLDL induced upregulation of SREBP-1 via NLRP3 inflammasome activation

A number of studies have shown that oxLDL activates NLRP3

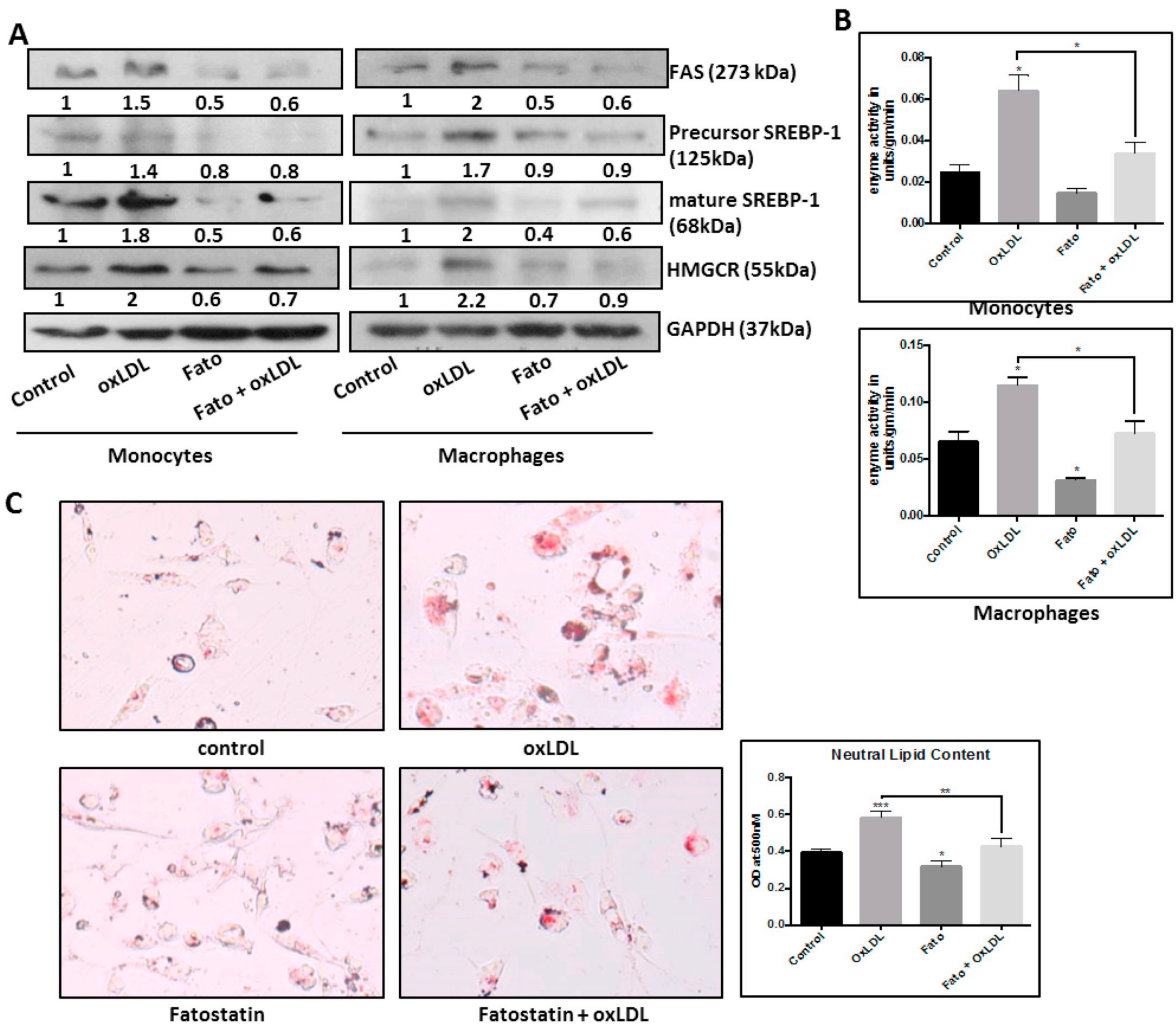

Fig 3. SREBP-1 inhibition prevented oxLDL induced lipid accumulation, critical component of foam cell formation: (A) Representative Western blot images of precursor SREBP-1, mature SREBP-1, FAS and HMGCR in monocytes and MDMs stimulated with oxLDL with and without fatostatin (fato) for 24 h. Numbers below the bands indicate fold change. (B) Representative bar diagrams show enzyme activity of FAS in monocytes and MDMs after 24 h of oxLDL stimulation. (C) ORO staining of oxLDL-stimulated MDMs with and without fatostatin (fato) for 24 h. Images captured at 200X magnification. The representative bar diagram for neutral lipid accumulation determined by isopropanol method of dye elution in the treatment groups *$p < .05$, **$p < .005$, ***$p < .0005$ vs respective controls.

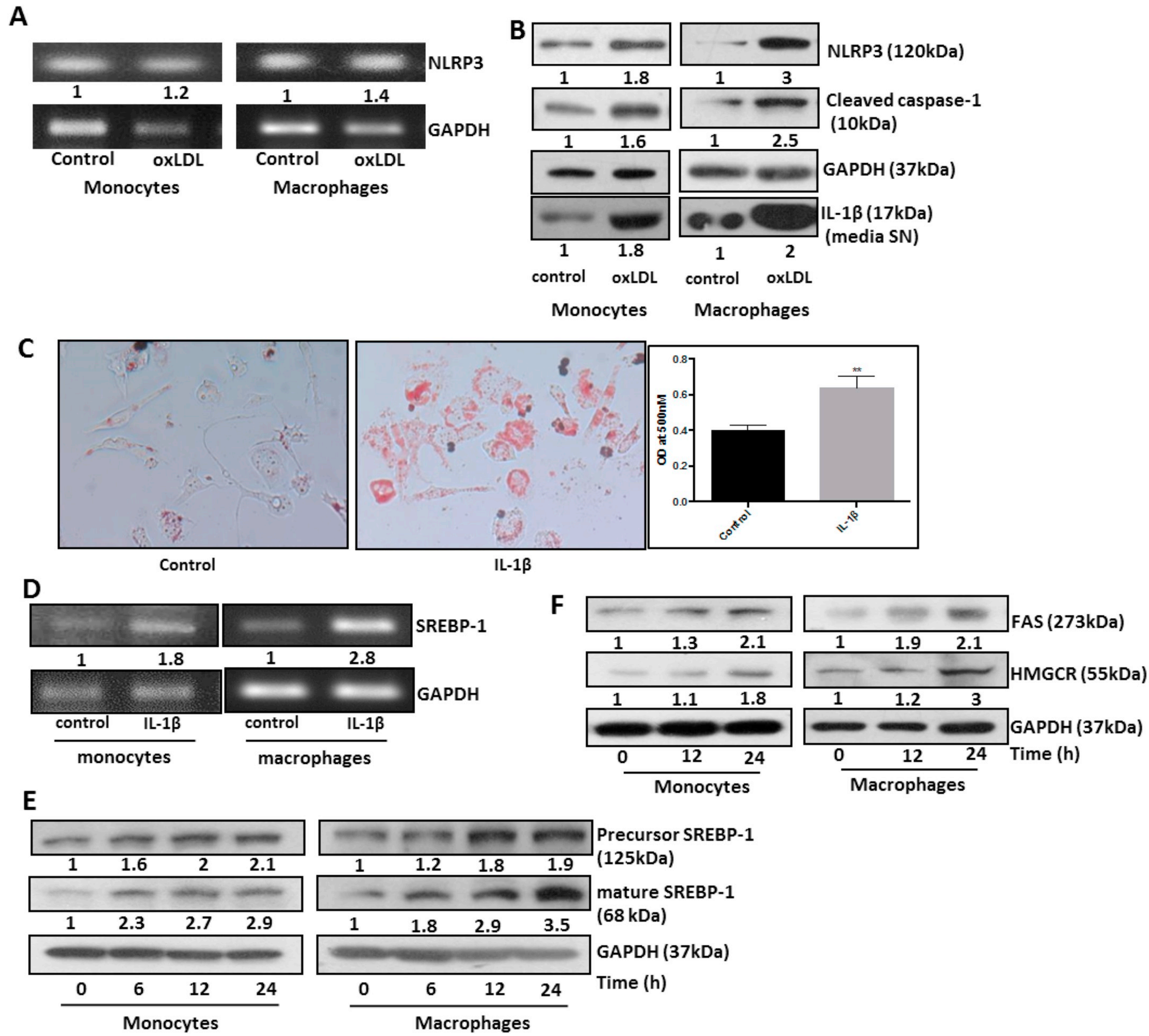

Fig 4. OxLDL-induced upregulation of SREBP-1 mediated by NLRP3 inflammasome activation: (A) Representative PCR images of NLRP3 mRNA expression with GAPDH as loading control shown in monocytes and MDMs stimulated with oxLDL for 16 h. (B) Representative Western blot images of proteins associated with inflammasome complex NLRP3 and cleaved caspase-1 in cell lysates along with IL-1β in media supernatant in monocytes and MDMs stimulated with oxLDL for 6 h are shown. (C) Representative ORO staining images in MDMs stimulated with IL-1β for 24 h shown, magnification 200X. Corresponding analysis of neutral lipid accumulation through dye elution using isoporpanol is represented as bar diagrams $^{**}p < .005$ vs control. (D) Representative PCR image of SREBP-1 mRNA expression with GAPDH as loading control shown in monocytes and MDMs stimulated with IL-1β for 16 h. (E) Representative Western blot images showing expression of precursor and mature SREBP-1 with GAPDH as loading control in monocytes and MDMs stimulated with IL-1β for 6, 12 and 24 h. (F) Representative Western blotting images of FAS and HMGCR in monocytes and MDMs treated with IL-1β for 12 and 24 h are shown. Numbers below the blots show fold changes.

inflammasome in both monocytes and MDMs [18,26], we were interested in finding its role in SREBP-1 regulation. Therefore, we first assessed oxLDL-induced NLRP3 inflammasome in both cell types. As shown in Fig. 4A, we detected increased expression of NLRP3 at RNA level by 1.2-fold in monocytes and by 1.4-fold ($p < .05$) in MDMs at 16 h as compared to control. We further assessed NLRP3 protein in cell lysates and caspase-1, its downstream target, and IL-1β in the cell culture media after stimulation with oxLDL. As shown in Fig. 4B, in U937 monocytes, oxLDL exposure led to significant ($p < .05$) increase in NLRP3, caspase-1 (cleaved) and IL-1β by 1.8-, 1.6- and 1.8-fold, respectively, as compared to respective controls. Similarly, in MDMs NLRP3, cleaved caspase-1 and active IL-1β levels increased significantly ($p < .05$) by 3-, 2.5- and 2-fold, respectively as compared to respective controls (Fig. 4B).

Further, as per our hypothesis we next determined if the product of NLRP3 inflammasome activation, IL-1β, could enhance the lipid synthesizing machinery in MDMs. Thus, first we induced MDMs with 10 ng/ml of IL-1β for 24 h and assessed lipid accumulation ORO staining. As shown in Fig. 4C, the lipid accumulation significantly ($p < .005$) increased by 61.5% in IL-1β stimulated cells compared to control. Further, we measured the expression of SREBP-1 at RNA levels in IL-1β stimulated monocytes and MDMs and observed that it increased significantly ($p < .05$) to 1.8-fold in monocytes and 2.8-folds in MDMs, respectively as compared to respective controls (Fig. 4D). At protein level, a significant ($p < .005$) increase in the precursor form of SREBP-1 in monocytes by 1.6-, 2- and 2.1-fold at 6, 12 and 24 h, respectively and in mature SREBP-1 by 2.3-, 2.7- and 2.9-fold, respectively as compared to controls was observed (Fig. 4E). A similar pattern was also observed in MDMs after stimulation with IL-1β, where precursor SREBP-1 increased significantly ($p < .05$) by 1.2-, 1.8- and 1.9-fold, and mature form of SREBP-1 increased by 1.8-, 2.9- and 3.5- fold ($p < .005$) at 6, 12 and 24 h, respectively as compared to controls (Fig. 4E). In addition to this, we analyzed IL-1β-mediated effect on the downstream proteins such as lipid synthesizing enzymes FAS and HMGCR. In monocytes, FAS expression increased by 1.3- and 2.1-fold ($p < .005$) at 12 and 24 h, respectively; and in MDMs it increased by 1.9- and 2.1-fold ($p < .05$), respectively as compared to respective controls. The expression of HMGCR in monocytes increased significantly by 1.1- and 1.8-fold ($p < .05$); and in MDMs it increased by 1.2- and 3-fold ($p < .005$) at 12 and 24 h, respectively, as compared to respective controls.

3.5. OxLDL induced ROS-mediated NLRP3 inflammasome activation and upregulation of SREBP-1 and its downstream target proteins

The oxLDL is a well-known inducer of oxidative stress in cells and studies have shown that reactive oxygen species (ROS) activate NLRP3 inflammasome in different types of cells [27]. Therefore, we examined ROS levels using DCFDA assay. The fluorometric observations indicated a steady increase in ROS production by 1.2-, 1.5-, 1.8- and 2.3-fold ($p < .05$) in monocytes and in MDMs by 1.2-, 2.3-, 2.5- and 2.8-fold ($p < .05$) at different time points of 0, 30, 60 and 180 min, respectively compared to their respective controls (Fig. 5A(i-ii)).

Next, we examined whether oxLDL-induced ROS activated NLRP3 inflammasome and downstream effectors. The cells were stimulated with oxLDL for 6 h in the presence and absence of *N*-acetyl cysteine (NAC), an anti-oxidant and ROS quencher, and Western blotting was performed. As shown in Fig. 5B (left panel), NLRP3, cleaved caspase-1 and IL-1β levels increased by 2-, 2- and 1.5-fold ($p < .005$) in monocytes compared to respective controls upon oxLDL stimulation which decreased to near control values of 0.7-, 1.3- and 1-fold ($p < .05$) respectively in group pretreated with NAC before stimulation with oxLDL. In MDMs, NLRP3, cleaved caspase-1 and IL-1β increased by 2.7-, 2.3- and 1.4-fold ($p < .0005$) upon oxLDL stimulation which decreased to 1-, 1.2- and 0.8-fold ($p < .05$) respectively in group pretreated with NAC followed by oxLDL treatment (Fig. 5B, right panel).

We next studied the effect of ROS quenching by NAC on SREBP-1 and lipid synthesizing enzymes in monocytes. The levels of precursor and mature SREBP-1, FAS and HMGCR increased by 1.3-, 1.9-, 1.6- and 1.7-fold ($p < .05$) in oxLDL-treated group as compared to control, which decreased to 1.1-, 0.7-, 0.7- and 1.1-fold ($p < .05$) respectively in group pretreated with NAC before oxLDL stimulation (Fig. 5C, left panel). Further, in MDMS the precursor and mature SREBP-1, FAS and HMGCR levels increased by 1.4-, 2-, 1.6- and 2.7-fold ($p < .005$) upon stimulation with oxLDL as compared to control. In the group pretreated with NAC before oxLDL stimulation their levels decreased to near control values of 1.1-, 1.-, 0.9- and 1.4-fold ($p < .05$) respectively (Fig. 5C, right panel).

To further confirm that SREBP-1 activation occurs in NLRP3 -dependent manner, we silenced NLRP3 using siRNA in monocytes up to 70% ($p < .05$) (Fig. 5Di). The NLRP3 expression in scrambled siRNA-transfected cells increased to 1.8-fold upon oxLDL stimulation compared to unstimulated cells, whereas in NLRP3 silenced cells the levels of NLRP3 was only approximately 0.5-fold after oxLDL stimulation as compared to 0.4-fold in unstimulated cells. Further, expression of mature SREBP-1 increased to 1.9-fold upon oxLDL stimulation which decreased to near control value of 1.1-fold ($p < .05$) in NLRP3 silenced cells induced with oxLDL up to 24 h (Fig. 5Dii).

4. Discussion

The presence of various endogenous stress molecules in circulation instigates an inflammatory response which leads to plaque buildup in the arteries [28]. The levels of circulating LDL and its tendency to undergo oxidation into oxLDL increases during metabolic syndrome. Although monocytes respond to the elevated metabolic stressors, they tend to proliferate and increase in number at the lesion sites and differentiate into macrophages. These macrophages further transform into foam cells by accumulating excessive lipids in their cytosol which compromises their migratory properties, and ability to resolve inflammation and instead contributes towards plaque formation and progression [29]. In our study oxLDL increased the viability of monocytes dose- and time-dependently, however higher doses of oxLDL and prolonged exposure was cytotoxic to MDMs. As derived from U937 monocytes after PMA-induced differentiation, MDMs do not proliferate further, and thus respond to oxLDL stimulation differently than monocytes by undergoing cell death. Indeed, dead macrophages have been observed in the atherosclerotic plaques [30]. Studies have shown that excessive uptake of lipids through overexpressed scavenger receptors and decrease in the cholesterol efflux *via* downregulation of cholesterol efflux proteins are some of the primary causes for FCF [31–33]. However, it is not clear if lipid homeostasis deregulation is limited only to uptake of lipids or whether skewed lipid synthesis in macrophages also acts as an important contributor to FCF. Therefore, to find an answer, we explored the cellular signaling that could regulate *de novo* lipid synthesis in monocytes and MDMs in the presence of oxLDL.

The oxLDL contains enormous amount of oxysterols, where certain oxysterols have been shown to inhibit cholesterol efflux proteins [34]. It is likely that the oxidatively modified oxysterols do not get identified by the sterol sensors of the cells which may be perceived as deficient level of sterol by the cells. To compensate this deficiency, cells promote *de novo* lipid synthesis in the backdrop of overloaded modified oxysterols. To understand this further we first measured the expression and activation of SREBP-1, a critical regulator of lipid homeostasis in the cells. Stimulation of monocytes and MDMs with oxLDL upregulated the expression of SREBP-1 both at transcriptional and translational levels, and in a time-dependent manner, which suggests that oxLDL regulates SREBP-1, the transcription factor for lipid synthesis genes.

SREBPs (125 kDa protein) are basic helix-loop-helix leucine zipper family of transcription factors that control lipid synthesis and homeostasis [13]. They are synthesized as inactive precursors bound to the endoplasmic reticulum along with an escort protein SREBP cleavage activating protein (SCAP), and another protein, insulin induced gene (INSIG) which together acts as a sensor for cytosolic sterol levels [15]. INSIG-SCAP interaction weakens during low cytosolic sterol levels that lead to the translocation of SCAP-SREBP to Golgi apparatus, where SREBP undergoes proteolytic cleavage into mature SREBP consisting of the N-terminal domain (now a 68 kDa protein) which acts as an active transcription factor. It activates the target genes by binding to the sterol response elements [35,36]. In concert with this, we observed increased nuclear translocation of mature SREBP-1 in the presence of oxLDL. SREBP-1 regulates both fatty acid and cholesterol synthesis, and it was confirmed by our observation of increased expression of its two downstream proteins FAS and HMGCR, which are responsible for synthesis of fatty acid and cholesterol, respectively. Further, to ascertain that oxLDL-induced activation of SREBP-1 could indeed increase FAS and HMGCR expression and enhanced lipid accumulation in monocytes and MDMs, we used fatostatin, a known chemical inhibitor of SREBP-1. Fatostatin, when given prior to stimulation with oxLDL, significantly prevented SREBP-1 level as well as its downstream target proteins, FAS and HMGCR (Fig. 3A). Fatostatin also decreased the level of lipid accumulation, which suggest that oxLDL activates *de novo* lipid synthesis in monocytes and MDMs *via* SREBP-1 leading to increased lipid accumulation.

We next investigated the cellular signaling through which oxLDL could promote lipid synthesizing machinery in the monocytes and MDMs. The oxLDL is known for its oxidative stress and inflammation promoting abilities [17]. Recently, they have also been identified as potent activators of inflammasome in monocytes and MDMs [18]. Thus, we examined whether oxLDL-induced activation of NLRP3 inflammasome, and subsequent release of IL-1β could promote new lipid synthesis and MDMs conversion into foam cells. We report here that oxLDL stimulation of monocytes and MDMs increased the expression as well as

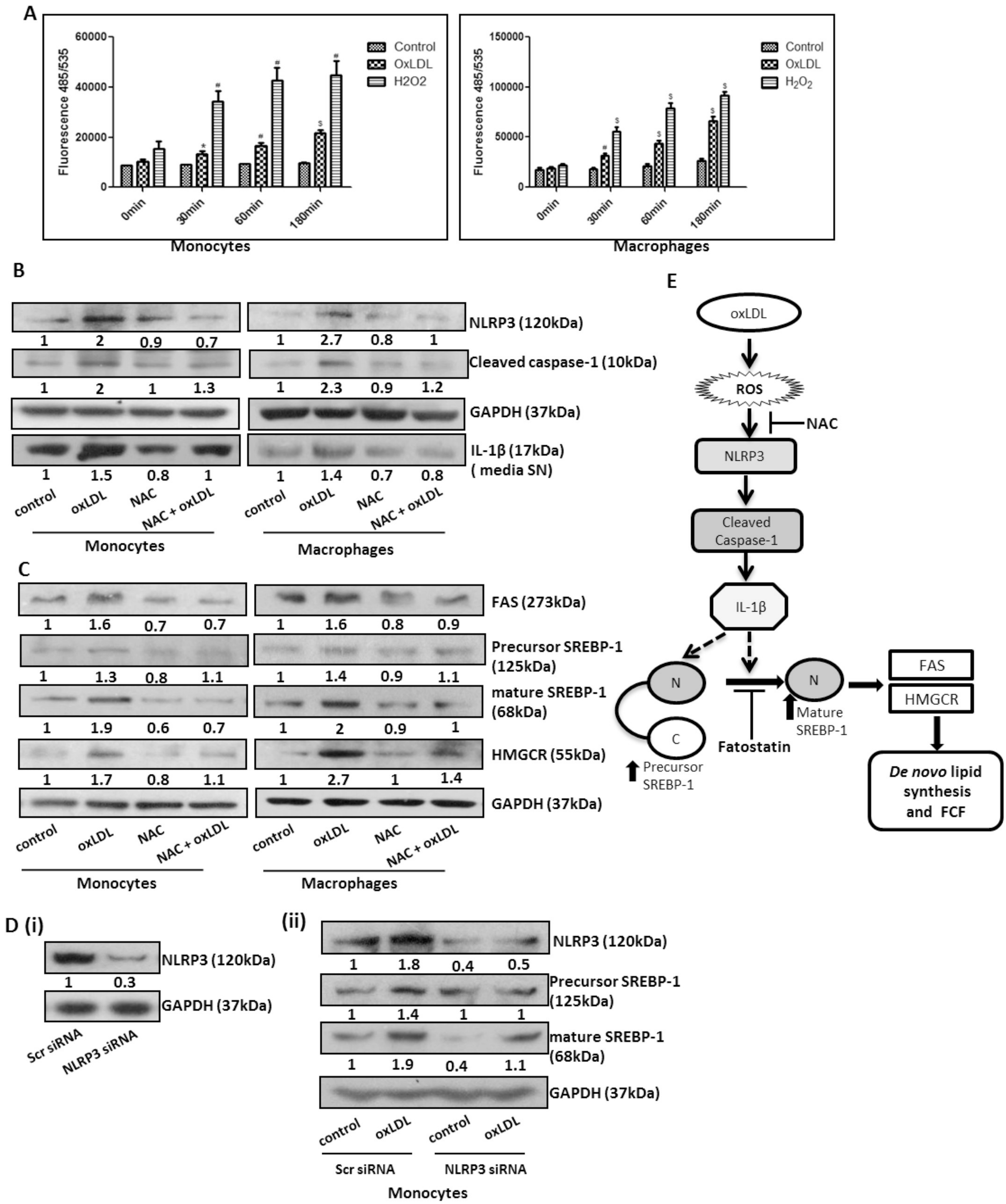

(caption on next page)

Fig. 5. OxLDL induced ROS mediated NLRP3 inflammasome activation, and upregulation of SREBP-1 and its downstream target proteins (A) DCFDA assay to detect ROS production was performed in monocytes and MDMs treated with oxLDL and 1mM of H_2O_2 (positive control) for varied time points (min), the data represented as bar diagrams (n = 3),*p < .5, #p < .005, $p < .0005 versus respective controls. (B) Representative Western blotting images of inflammasome associated proteins NLRP3, cleaved caspase-1 along with GAPDH as loading control in whole cells lyastes and IL-1β in media supernatant of monocytes and MDMs treated with oxLDL, NAC and pretreated with NAC before oxLDL stimulation for 6 h are shown numbers below the blot represent fold change. (C) Western blot images of precursor and mature SREBP-1, FAS and HMGCR with GAPDH as loading control in monocytes and MDMs stimulated with oxLDL with and without NAC for 24 h are shown. (D) Western blot image of (i) NLRP3 after knockdown using siRNA by the end of 72 h of transfection, (ii) NLRP3, precursor and mature SREBP-1 after silencing NLRP3 in monocytes followed by stimulation with oxLDL for 24 h. (E) Schematic Diagram showing oxLDL induce marcophage FCF via ROS/NLRP3/IL-1β/ SREBP-1/FAS-HMGCR: oxLDL induce ROS production in monocytes and MDMs which leads to NLRP3 inflammasome activation along with caspase-1, followed by IL-1β production. IL-1β increases precursor and mature form of SREBP-1 along with the nuclear translocation of the same. SREBP-1 further upregulates the lipid synthesizing proteins leading to *de novo* lipid synthesis and FCF.

activation of NLRP3, increased cleaved caspase-1 and IL-1β in both monocytes and MDMs. Previous studies have shown that in IL-1β$^{-/-}$ ApoE$^{-/-}$ mice fed with high-fat diet did not show macrophage foam cell phenotype [18,37] implicating the role of IL-1β in FCF. Further, evidences indicate that IL-1β promotes FCF in macrophages *via* upregulation of CD-36 cell surface receptor and *via* downregulating the expression of efflux transporters such as ABCA1 and ABCG1 [18,38], however, its role in *de novo* lipid synthesis remains elusive. Since oxLDL enhanced the release of IL-1β in both the cell types, to further explore its role in *de novo* lipid synthesis we induced the cells directly with IL-1β and observed that IL-1β upregulated the mRNA and protein levels of SREBP-1. Further, an increase in the precursor and mature forms of SREBP-1, as well as in its downstream target genes FAS and HMGCR expression were observed in both the cell types. Furthermore, ORO staining of IL-1β stimulated MDMs strongly suggested that oxLDL could induce enhanced lipid accumulation and resultant FCF through IL-1β. It is likely that once released in active form, IL-1β initiates an autocrine and paracrine cellular signaling which enacts oxLDL-mediated FCF. IL-1β is known to act by binding to IL-1β receptors on target cells followed by activation and recruitment of varied signaling molecules such as myeloid differentiation factor 88 (MyD88), IL-1 receptor-associated kinase 4 (IRAK4) and TNF receptor-associated factor 6 (TRAF6). Signaling through these molecules activates NF-κB as well as other MAP kinase pathways [39]. Studies also indicate that activation of SREBP in LPS-induced macrophages is found to occur *via* cross talk between NF-κB and SCAP which readily escorts SREBP to the nucleus [40], hence activation of IL-1β/MyD88/NF-κB/SREBP signaling pathway could be a likely signaling which contributes towards *de novo* lipid synthesis and FCF.

So far, we have observed that oxLDL could activate SREBP-1 and its downstream lipid synthesizing enzymes through NLRP3-mediated release of IL-1β, however, the mechanism of NLRP3 activation by oxLDL remained elusive. Further, ROS has been shown to induce NLRP3 inflammasome in many cells [27]. We also observed an increased ROS production in monocytes and MDMs upon oxLDL stimulation. The quenching of ROS by NAC decreased oxLDL-induced inflammasome activation as well as other associated proteins and SREBP-1 and lipid synthesizing enzymes FAS and HMGCR. We further examined the role NLRP3 in oxLDL-induced SREBP-1 activation by siRNA-mediated silencing of NLRP3 in monocytes. The oxLDL stimulation of NLRP3-silenced monocytes resulted in decreased level of mature SREBP-1 expression compared to similarly stimulated monocytes transfected with scrambled siRNA. These results indicated that oxLDL could activate SREBP-1 and increased lipid synthesis *via* ROS-mediated NLRP3 activation and subsequent release of IL-1β. There are several other signaling molecules such as AMPK and LXR which can also be critical links between IL-1β and SREBP-1 [21,41], and need to be further investigated.

5. Conclusion

The results in this study have shown for the first time that oxLDL could activate lipid homeostasis regulator SREBP-1 and its target genes FAS and HMGCR, increase *de novo* lipid synthesis and promote lipid accumulation in macrophages *via* ROS-mediated NLRP3 activation and release of IL-1β (Fig. 5E). These results suggest that SREBP-1 modulation may be an innovative approach to inhibit lipid accumulation in oxLDL-induced macrophages which is an initial event in atherosclerotic plaque formation.

Author contributions

The work was conceived and designed by UCSY and JFV. The experimental work was carried out by JFV and RP. All the authors were involved in data analysis and writing the manuscript.

Acknowledgments

This work was supported and funded by Gujarat State Biotechnology Mission (GSBTM) (GSBTM/MD/PROJECTS/SSA/5050/2016-17), Govt. of Gujarat, India. Junior Research Fellowship (JRF) to JFV from GSBTM, Govt. of Gujarat and to RP from SERB, Government of India and award of Ramanujan fellowship by SERB/DST to UCSY are thankfully acknowledged.

Declaration of interest

None.

References

[1] D. Mozaffarian, E.J. Benjamin, A.S. Go, D.K. Arnett, M.J. Blaha, M. Cushman, et al., Heart disease and stroke statistics–2015 update: a report from the American Heart Association, Circulation 131 (4) (2015) e29–322.
[2] J.C. Fruchart, M.C. Nierman, E.S. Stroes, J.J. Kastelein, P. Duriez, New risk factors for atherosclerosis and patient risk assessment, Circulation 109 (23 Suppl 1) (2004) III15–9.
[3] E. Di Angelantonio, N. Sarwar, P. Perry, S. Kaptoge, K.K. Ray, A. Thompson, et al., Major lipids, apolipoproteins, and risk of vascular disease, JAMA 302 (18) (2009) 1993–2000.
[4] D. Steinberg, S. Parthasarathy, T.E. Carew, J.C. Khoo, J.L. Witztum, Beyond cholesterol. Modifications of low-density lipoprotein that increase its atherogenicity, N. Engl. J. Med. 320 (14) (1989) 915–924.
[5] M.O. Pentikainen, K. Oorni, M. Ala-Korpela, P.T. Kovanen, Modified LDL - trigger of atherosclerosis and inflammation in the arterial intima, J. Intern. Med. 247 (3) (2000) 359–370.
[6] N. Leitinger, Oxidized phospholipids as triggers of inflammation in atherosclerosis, Mol. Nutr. Food Res. 49 (11) (2005) 1063–1071.
[7] D. Steinberg, Atherogenesis in perspective: hypercholesterolemia and inflammation as partners in crime, Nat. Med. 8 (11) (2002) 1211–1217.
[8] B. Fuhrman, A. Partoush, N. Volkova, M. Aviram, Ox-LDL induces monocyte-to-macrophage differentiation in vivo: possible role for the macrophage colony stimulating factor receptor (M-CSF-R), Atherosclerosis 196 (2) (2008) 598–607.
[9] K.J. Moore, F.J. Sheedy, E.A. Fisher, Macrophages in atherosclerosis: a dynamic balance, Nat Rev Immunol 13 (10) (2013) 709–721.
[10] V.V. Kunjathoor, M. Febbraio, E.A. Podrez, K.J. Moore, L. Andersson, S. Koehn, et al., Scavenger receptors class A-I/II and CD36 are the principal receptors responsible for the uptake of modified low density lipoprotein leading to lipid loading in macrophages, J. Biol. Chem. 277 (51) (2002) 49982–49988.
[11] I.A. Zani, S.L. Stephen, N.A. Mughal, D. Russell, S. Homer-Vanniasinkam, S.B. Wheatcroft, et al., Scavenger receptor structure and function in health and disease, Cell 4 (2) (2015) 178–201.
[12] M. Westerterp, K. Tsuchiya, I.W. Tattersall, P. Fotakis, A.E. Bochem, M.M. Molusky, et al., Deficiency of ATP-Binding Cassette Transporters A1 and G1 in Endothelial Cells Accelerates Atherosclerosis in mice, Arterioscler. Thromb. Vasc. Biol. 36 (7) (2016) 1328–1337.

[13] D. Eberle, B. Hegarty, P. Bossard, P. Ferre, F. Foufelle, SREBP transcription factors: master regulators of lipid homeostasis, Biochimie 86 (11) (2004) 839–848.

[14] L.M. Perez-Belmonte, I. Moreno-Santos, F. Cabrera-Bueno, G. Sanchez-Espin, D. Castellano, M. Such, et al., Expression of Sterol Regulatory Element-Binding Proteins in epicardial adipose tissue in patients with coronary artery disease and diabetes mellitus: preliminary study, Int. J. Med. Sci. 14 (3) (2017) 268–274.

[15] M.S. Brown, J.L. Goldstein, The SREBP pathway: regulation of cholesterol metabolism by proteolysis of a membrane-bound transcription factor, Cell 89 (3) (1997) 331–340.

[16] Z. Chen, M. Martin, Z. Li, J.Y.J. Shyy, Endothelial Dysfunction: the Role of SREBP-Induced NLRP3 Inflammasome in Atherosclerosis, Curr. Opin. Lipidol. 25 (5) (2014) 339–349.

[17] J.F. Varghese, R. Patel, U.C.S. Yadav, Novel insights in the metabolic syndrome-induced oxidative stress and inflammation-mediated atherosclerosis, Curr. Cardiol. Rev. 14 (1) (2018) 4–14.

[18] W. Liu, Y. Yin, Z. Zhou, M. He, Y. Dai, OxLDL-induced IL-1 beta secretion promoting foam cells formation was mainly via CD36 mediated ROS production leading to NLRP3 inflammasome activation, Inflamm. Res. 63 (1) (2014) 33–43.

[19] H. Shintani, LDL Isolation and Copper-Catalysed Oxidation, Pharmaceutica Analytica Acta 4 (6) (2013) 247.

[20] J. Galle, C. Wanner, Oxidized LDL and Lp(a). Preparation, modification, and analysis, Methods Mol. Biol. 108 (1998) 119–130.

[21] D.K. Nambiar, G. Deep, R.P. Singh, C. Agarwal, R. Agarwal, Silibinin inhibits aberrant lipid metabolism, proliferation and emergence of androgen-independence in prostate cancer cells via primarily targeting the sterol response element binding protein 1, Oncotarget 5 (20) (2014) 10017–10033.

[22] D. Tailor, E.R. Hahm, R.K. Kale, S.V. Singh, R.P. Singh, Sodium butyrate induces DRP1-mediated mitochondrial fusion and apoptosis in human colorectal cancer cells, Mitochondrion 16 (2014) 55–64.

[23] C.V. Kavitha, C. Agarwal, R. Agarwal, G. Deep, Asiatic acid inhibits pro-angiogenic effects of VEGF and human gliomas in endothelial cell culture models, PLoS One 6 (8) (2011) e22745.

[24] U.C. Yadav, K. Moorthy, N.Z. Baquer, Effects of sodium-orthovanadate and Trigonella foenum-graecum seeds on hepatic and renal lipogenic enzymes and lipid profile during alloxan diabetes, J. Biosci. 29 (1) (2004) 81–91.

[25] P. Tontonoz, L. Nagy, J.G. Alvarez, V.A. Thomazy, R.M. Evans, PPARgamma promotes monocyte/macrophage differentiation and uptake of oxidized LDL, Cell 93 (2) (1998) 241–252.

[26] W.L. Li, L.G. Hua, P. Qu, W.H. Yan, C. Ming, Y.D. Jun, et al., NLRP3 inflammasome: a novel link between lipoproteins and atherosclerosis, Arch. Med. Sci. 12 (5) (2016) 950–958.

[27] J.M. Abais, M. Xia, Y. Zhang, K.M. Boini, P.L. Li, Redox Regulation of NLRP3 Inflammasomes: ROS as Trigger or Effector? Antioxid. Redox Signal. 22 (13) (2015) 1111–1129.

[28] J.F. Bentzon, F. Otsuka, R. Virmani, E. Falk, Mechanisms of plaque formation and rupture, Circ. Res. 114 (12) (2014) 1852–1866.

[29] G.J. Randolph, Mechanisms that regulate macrophage burden in atherosclerosis, Circ. Res. 114 (11) (2014) 1757–1771.

[30] K.J. Moore, I. Tabas, The Cellular Biology of Macrophages in Atherosclerosis, Cell 145 (3) (2011) 341–355.

[31] T.J. van Berkel, R. Out, M. Hoekstra, J. Kuiper, E. Biessen, M. van Eck, Scavenger receptors: friend or foe in atherosclerosis? Curr. Opin. Lipidol. 16 (5) (2005) 525–535.

[32] H.Y. Huh, S.F. Pearce, L.M. Yesner, J.L. Schindler, R.L. Silverstein, Regulated expression of CD36 during monocyte-to-macrophage differentiation: potential role of CD36 in foam cell formation, Blood 87 (5) (1996) 2020–2028.

[33] L. Yvan-Charvet, M. Ranalletta, N. Wang, S. Han, N. Terasaka, R. Li, et al., Combined deficiency of ABCA1 and ABCG1 promotes foam cell accumulation and accelerates atherosclerosis in mice, J. Clin. Invest. 117 (12) (2007) 3900–3908.

[34] I.C. Gelissen, A.J. Brown, E.L. Mander, L. Kritharides, R.T. Dean, W. Jessup, Sterol efflux is impaired from macrophage foam cells selectively enriched with 7-ketocholesterol, J. Biol. Chem. 271 (30) (1996) 17852–17860.

[35] L.P. Sun, L. Li, J.L. Goldstein, M.S. Brown, Insig required for sterol-mediated inhibition of Scap/SREBP binding to COPII proteins in vitro, J. Biol. Chem. 280 (28) (2005) 26483–26490.

[36] M. Amemiya-Kudo, H. Shimano, A.H. Hasty, N. Yahagi, T. Yoshikawa, T. Matsuzaka, et al., Transcriptional activities of nuclear SREBP-1a, −1c, and −2 to different target promoters of lipogenic and cholesterogenic genes, J. Lipid Res. 43 (8) (2002) 1220–1235.

[37] H. Kirii, T. Niwa, Y. Yamada, H. Wada, K. Saito, Y. Iwakura, et al., Lack of interleukin-1beta decreases the severity of atherosclerosis in ApoE-deficient mice, Arterioscler. Thromb. Vasc. Biol. 23 (4) (2003) 656–660.

[38] M. Chen, W. Li, N. Wang, Y. Zhu, X. Wang, ROS and NF-kappaB but not LXR mediate IL-1beta signaling for the downregulation of ATP-binding cassette transporter A1, Am J Physiol Cell Physiol 292 (4) (2007) C1493–C1501.

[39] G. Schett, J.M. Dayer, B. Manger, Interleukin-1 function and role in rheumatic disease, Nat. Rev. Rheumatol. 12 (1) (2016) 14–24.

[40] L.C. Li, Z. Varghese, J.F. Moorhead, C.T. Lee, J.B. Chen, X.Z. Ruan, Cross-talk between TLR4-MyD88-NF-kappaB and SCAP-SREBP2 pathways mediates macrophage foam cell formation, Am. J. Physiol. Heart Circ. Physiol. 304 (6) (2013) H874–H884.

[41] T. Yoshikawa, H. Shimano, N. Yahagi, T. Ide, M. Amemiya-Kudo, T. Matsuzaka, et al., Polyunsaturated fatty acids suppress sterol regulatory element-binding protein 1c promoter activity by inhibition of liver X receptor (LXR) binding to LXR response elements, J. Biol. Chem. 277 (3) (2002) 1705–1711.